

Available online at [www.sciencedirect.com](http://www.sciencedirect.com)**ScienceDirect**

Procedia Engineering 127 (2015) 1048 – 1055

**Procedia  
Engineering**[www.elsevier.com/locate/procedia](http://www.elsevier.com/locate/procedia)

International Conference on Computational Heat and Mass Transfer-2015

# Mixed Convective Heat and Mass Transfer Flow of Nanofluids in Concentric Annulus

G. Sreedevi<sup>a,\*</sup>, R. Raghavendra Rao<sup>b</sup>, A.J. Chamkha<sup>c</sup>, D.R.V. Prasada Rao<sup>d</sup><sup>a,b</sup>Department of Mathematics, K.L. University, Green Fields, Vaddeswaram, Guntur 522502, A.P, India<sup>c</sup>Mechanical Engineering Department, Prince Mohammad Bin Fahd University (PMU), Al-Khobar, 31952, Kingdom of Saudi Arabia<sup>d</sup>Department of Mathematics, S.K. University, Anantapur-515003, A.P, India

## Abstract

This paper studies the non-Darcy natural convective heat transfer flow of nanofluid flow through a porous medium in a co-axial cylindrical duct where the boundaries are maintained at constant temperature and concentration. The flow in the porous material is given by a linear Brinkman-Forchheimer-extended Darcy equation. The Boussinesq approximation is invoked so that the effect of density variation is combined to the buoyancy forces. The equations of momentum, energy and diffusion are coupled and linear. Galerkin finite element analysis is employed with quadratic polynomial approximations. At different axial positions, analysis is conducted for the behaviour of velocity, temperature and concentration.

© 2015 The Authors. Published by Elsevier Ltd. This is an open access article under the CC BY-NC-ND license

(<http://creativecommons.org/licenses/by-nc-nd/4.0/>).

Peer-review under responsibility of the organizing committee of ICCHMT – 2015

**Keywords:** Mixed convection; Chemical reaction; Heat source absorption; Heat and Mass transfer; Nanofluid; Concentric annulus.

## 1. Introduction

By adding nanoscaled solid particles in a conventional cooling liquid, such as water and ethylene glycol the resulting suspension is referred as nanofluid has been explained by Choi and Eastman [1]. Viscous dissipation and the effect of buoyancy was analyzed by Antonio [2] in a vertical cylinder duct having laminar flow and heat transfer. El-Shaarawi and Al-Nimir [3] and Al-Nimir [4] have discussed the limiting case of fully developed natural

\* Corresponding author. Tel.: +91-988-553-9520; fax: +91-863-238-8999.

E-mail address: [sreedevihari2007@gmail.com](mailto:sreedevihari2007@gmail.com)

convection in porous annuli and were solved analytically for steady and transient cases. The solutions for the annular porous media valid for low modified Reynolds number was obtained by Philip [5].

The heat transfer deterioration in  $\text{Al}_2\text{O}_3$ -water and water-based copper oxide (CuO-water) nanofluids (with volume fraction 1% and 4%) has been absorbed experimentally by Putra et al. [6]. The natural convection of  $\text{TiO}_2$ -water in a vessel composed of two discs has been observed by Wen and Ding [7]. The natural heat convection deterioration in 0.5% ~ 6%  $\text{Al}_2\text{O}_3$ -water nanofluids has been reported by Li and Peterson [8]. From the experiments for 1.08%  $\text{Al}_2\text{O}_3$ -water nanofluid in a Rayleigh-Bénard configuration Rui et al. [9] has found deterioration in natural convection. Nnanna's [10] experiment depicts that the presence of  $\text{Al}_2\text{O}_3$  nanoparticles did not impede the water-free heat convection with the volume fraction in the range of 0.2% ~ 2%. The mixed convection flow in single and double-lid driven square cavities filled with water- $\text{Al}_2\text{O}_3$  nanofluid has been studied by Chamkha and Abu-Nada [11]. Taking variable thermal conductivity around a vertical cone in porous media Ghalambaz et al. [12] have analyzed the effects of nanoparticles diameter and concentration on natural convection of the  $\text{Al}_2\text{O}_3$ -water nanofluids. The natural heat convection of water-based alumina ( $\text{Al}_2\text{O}_3$ -water) nanofluids (with volume fraction 1% and 4%) in a horizontal cylinder has been observed numerically by Xiangyin Meng and Yan Li [13] and found that the temperature-dependent solver is better for water and 1%  $\text{Al}_2\text{O}_3$ -water nanofluid cases, while the original solver is better for 4%  $\text{Al}_2\text{O}_3$ -water nanofluid cases.

In this paper, we investigate non-Darcy convective heat transfer flow of a nanofluid in a cylindrical annulus by employing Galerkin method with quadratic polynomial approximation. The effect of various parameters on all the flow characteristics has been investigated.

## 2. Formulation of the problem

We consider the fully developed, steady laminar mixed convective flow of an incompressible viscous, electrically conducting fluid through a porous medium in the annular region between two vertical co-axial circular pipes. We choose the cylindrical polar co-ordinates system  $O(r, \theta, z)$  with the inner and outer cylinders at  $r = a$  and  $r = b$  respectively. The fluid is subjected to the influence of a radial magnetic field ( $H_0/r$ ). Pipes being sufficiently long all the physical quantities are independent of the axial co-ordinate  $z$ . The fluids are chosen to be of small conductivity so that the magnetic Reynolds number is much smaller than unity and hence the induced magnetic field is negligible compared to the applied radial field. Also the motion being rotationally symmetric the azimuthal velocity  $v$  is zero.

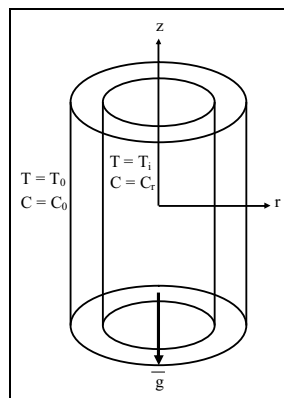


Fig. 1. Schematic diagram of the configuration

The Brinkman-Forchheimer-extended Darcy model which accounts for the inertia and boundary effects has been used for the momentum equation in the porous region. The equations of motion governing the MHD flow through the porous medium are

$$-\frac{\partial p}{\partial z} + \frac{\mu_{nf}}{\delta \rho_{nf}} \left( \frac{\partial^2 u}{\partial r^2} + \frac{1}{r} \frac{\partial u}{\partial r} \right) - \frac{\mu_{nf}}{\rho_{nf} k} u - \frac{\delta F}{\sqrt{k}} u^2 + (\rho \beta)_{nf} (T - T_i) - (\sigma \mu_e^2 H_0^2 / r^2) u = 0 \quad (1)$$

$$(\rho C_p)_{nf} u \frac{\partial T}{\partial z} = k_{nf} \left( \frac{\partial^2 T}{\partial r^2} + \frac{1}{r} \frac{\partial T}{\partial r} \right) + Q(T - T_i) \quad (2)$$

$$u \frac{\partial C}{\partial z} = D_B \left( \frac{\partial^2 C}{\partial r^2} + \frac{1}{r} \frac{\partial C}{\partial r} \right) - k_c' C \quad (3)$$

where  $u$  is the axial velocity in the porous region,  $T$ ,  $C$  are the temperature and concentration of the fluid,  $k$  is the permeability of porous medium,  $F$  is a function that depends on Reynolds number, the microstructure of the porous medium and  $D_B$  is the molecular diffusivity,  $\beta$  is the coefficient of the thermal expansion,  $C_p$  is the specific heat,  $\rho$  is density and  $g$  is gravity,  $k_{11}$  is the cross diffusivity. The relevant boundary conditions are

$$\begin{aligned} u = 0, \quad T = T_i, \quad C = C_i \quad \text{at } r = a \\ u = 0, \quad T = T_0, \quad C = C_0 \quad \text{at } r = a + s \end{aligned} \quad (4)$$

The axial temperature and concentration gradients  $\frac{\partial T}{\partial z}$  &  $\frac{\partial C}{\partial z}$  are assumed to be constant, say,  $A$  &  $B$  respectively.

The properties of nanofluid are defined as follows

$$\begin{aligned} \alpha_{nf} &= \frac{k_{nf}}{(\rho C_p)_{nf}}, \mu_{nf} = \frac{\mu_f}{(1-\phi)^{2.5}}, \rho_{nf} = (1-\phi)\rho_f + \phi\rho_s \\ (\rho\beta)_{nf} &= (1-\phi)(\rho\beta)_f + \phi(\rho\beta)_s, (\rho C_p)_{nf} = (1-\phi)(\rho C_p)_f + \phi(\rho C_p)_s, \\ k_{nf} &= k_f \left( \frac{k_s + 2k_f - 2\phi(k_f - k_s)}{(k_s + 2k_f + 2\phi(k_f - k_s))} \right) \end{aligned} \quad (5)$$

The non-dimensional variables are as follows

$$z^* = \frac{z}{a}, \quad r^* = \frac{r}{a}, \quad u^* = \frac{a}{\gamma} u, \quad p^* = \frac{pa\delta}{(\rho)_f \gamma^2}, \quad \theta^* = \frac{T - T_i}{T_0 - T_i}, \quad s^* = \frac{s}{a}, \quad C^* = \frac{C - C_i}{C_0 - C_i} \quad (6)$$

From the above variables, the governing equations in the non-dimensional form are given, by removing the stars, along with the each parameter representation below.

$$\frac{1}{A_1 A_3} \left( \frac{\partial^2 u}{\partial r^2} + \frac{1}{r} \frac{\partial u}{\partial r} \right) = \pi + \frac{1}{A_1 A_3} \delta (D^{-1} + \frac{M^2 A_1}{r^2}) u + \delta^2 (D^{-1})^{1/2} \Delta u^2 - \frac{\delta G A_4}{A_2 A_3} \delta G(\theta) \quad (7)$$

$$\frac{A_2}{Pr} \left( \frac{\partial^2 \theta}{\partial r^2} + \frac{1}{r} \frac{\partial \theta}{\partial r} \right) = A_3 u N_t + \frac{\alpha}{Pr} \theta \quad (8)$$

$$\left(\frac{\partial^2 C}{\partial r^2} + \frac{1}{r} \frac{\partial C}{\partial r}\right) - \gamma C = Sc N_c u \quad (9)$$

$\Delta = FD^{-1}$  is Inertia parameter or Forchheimer number;  $G = \frac{g\beta(T_e - T_i)a^3}{\nu^2}$  is Grashof number;  $D^{-1} = \frac{a^2}{k}$  is

Inverse Darcy parameter;  $N_t = \frac{Aa}{T_1 - T_0}$  is non-dimensional temperature gradient;  $N_c = \frac{Ba}{C_1 - C_0}$  is non-dimensional

concentration gradient;  $Pr = \frac{\rho c_p \gamma}{\lambda}$  is Prandtl number;  $Sc = \frac{\nu}{D_1}$  is Schmidt number;

$$A_1 = \frac{1}{(1-\phi)^{2.5}}, A_2 = \frac{k_{nf}}{k_f}, A_3 = (1-\phi) + \phi\left(\frac{\rho_s}{\rho_f}\right), A_4 = (1-\phi) + \phi\left(\frac{(\rho\beta)_s}{(\rho\beta)_f}\right), A_5 = (1-\phi) + \phi\left(\frac{(\rho C_p)_s}{(\rho C_p)_f}\right),$$

The corresponding non-dimensional conditions are

$$\begin{aligned} u = 0, \quad \theta = 0, \quad C = 0 \quad \text{at } r = 1 \\ u = 0, \quad \theta = 1, \quad C = 1 \quad \text{at } r = 1 + s \end{aligned} \quad (10)$$

### 3. Method of solution

The Galerkin finite element analysis with quadratic polynomial approximation functions is carried out along the radial distance across the circular duct. For different variations in governing parameters, the behavior of the velocity, temperature and concentration profiles are discussed. The global coupled matrices for the velocity, temperature and concentration are obtained.

Assuming an arbitrary element  $ek$  and let  $u_k$ ,  $\theta_k$  and  $C_k$  be the values of  $u$ ,  $\theta$  and  $C$  in the element  $ek$ , the error residuals are defined as

$$E_P^k = \frac{1}{A_1 A_3} \frac{d}{dr} \left( r \frac{du^k}{dr} \right) + \frac{\delta G A_4}{A_2 A_3} (\theta^k) - \frac{1}{A_1 A_3} \delta \left( D^{-1} + \frac{M^2}{r^2} \right) r u^k - \delta^2 \Delta r (u^k)^2 \quad (11)$$

$$E_\theta^k = \frac{A_2}{Pr} \frac{d}{dr} \left( r \frac{d\theta^k}{dr} \right) - r N_t u^k + \frac{\alpha}{Pr} r \theta \quad (12)$$

$$E_C^k = \frac{d}{dr} \left( r \frac{dC^k}{dr} \right) - r Sc N_c u^k - \gamma C^k \quad (13)$$

These are expressed as linear combinations in terms of respective local nodal values.

$$u^k = u_1^k \psi_1^k + u_3^k \psi_1^k + u_3^k \psi_3^k, \theta^k = \theta_1^k \psi_1^k + \theta_2^k \psi_2^k + \theta_3^k \psi_3^k, C^k = C_1^k \psi_1^k + C_2^k \psi_2^k + C_3^k \psi_3^k \quad (14)$$

where  $\psi_1^k$ ,  $\psi_2^k$  etc are Lagrange's quadratic polynomials.

Galerkin's method is used to convert the partial differential Eqs. (11) – (13) into matrix form of equations which results into 3x3 local stiffness matrices. All these local matrices are assembled in a global matrix by substituting the global nodal values of order I.

The rate of heat and mass transfer is evaluated by using the following formulae. Nusselt number (rate of heat transfer) is calculated using the formula  $Nu = -\left(\frac{d\theta}{dr}\right)_{r=1,1+s}$ . Sherwood number (rate of mass transfer) is calculated

using the formula  $Sh = -\left(\frac{dC}{dr}\right)_{r=1,1+s}$ .

#### 4. Important conclusions and results in this analysis

Inverting the stiffness matrices and following iteration procedure the velocity, temperature and concentration have been evaluated for different values of  $M$ ,  $\alpha$ ,  $\gamma$  and  $\emptyset$ . The rate of heat and mass transfer has been calculated numerically on the boundaries. Numerical evaluations were performed and graphical results were obtained to illustrate the details of the flow and heat and mass transfer characteristics and their dependence on some physical parameters. The key findings are summarized below:

As the magnetic field parameter enhances, the momentum boundary layer thickness and the temperature reduces in the region, whereas in the case of copper-water nanofluid, concentration enhances in the entire flow region. In the case of  $Al_2O_3$ -water nanofluid, velocity reduces while the temperature and concentration enhances in the boundary layer as shown in Figs. 2a-2c. The values of velocity, temperature and concentration in the case of  $Al_2O_3$ -water nanofluid, is relatively higher than that of copper-water nanofluid.

The variation of heat transfer  $Nu$  with magnetic parameter  $M$ , higher the Lorentz force larger  $|Nu|$  on  $r=1$  and  $r=2$  in the case of copper-water nanofluid. But in the case of  $Al_2O_3$ -water nanofluid  $|Nu|$  enhances on  $r=1$  and reduces in  $r=2$  as shown in Table 1.

Figs. 3a-3c show the case of copper-water nanofluid, an increase in the strength of heat generating source enhances the velocity and concentration and reduces the temperature in both types of nanofluids.  $|Nu|$  enhances on  $r=1$  and  $r=2$  with increase in the strength of generating heat source. In the case of  $Al_2O_3$ -water nanofluid  $|Nu|$  reduces on  $r=1$  and enhances on  $r=2$  with increases in  $\alpha > 0$ ,  $|Nu|$  enhances on both the cylinders is represented in Table 1.

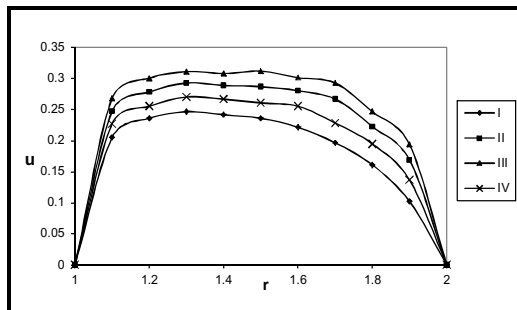


Fig. 2a. Variation of  $u$  with different values of  $M$  (5, 10) in Cu-water and  $Al_2O_3$ -water

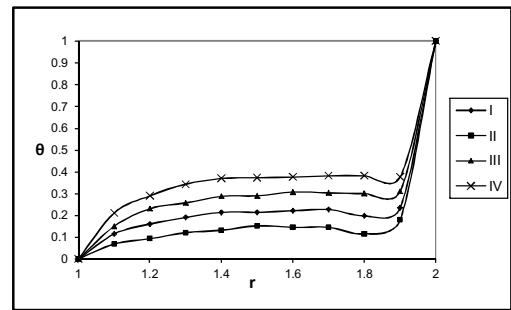


Fig. 2b. Variation of  $\theta$  with different values of  $M$  (5, 10) in Cu-water and  $Al_2O_3$ -water

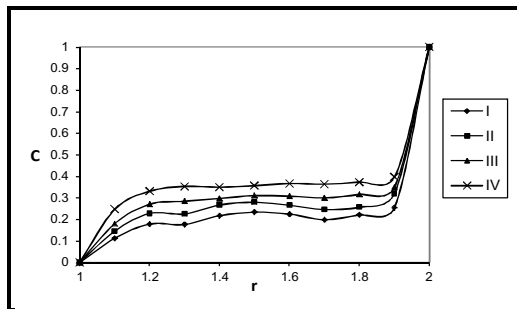


Fig. 2c. Variation of  $C$  with different values of  $M$  (5, 10) in Cu-water and  $Al_2O_3$ -water

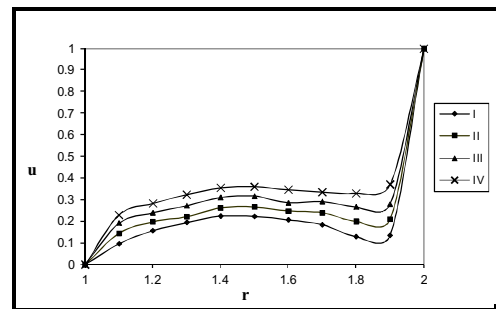


Fig. 3a. Variation of  $u$  with different values of  $\alpha$  (2, 4) in Cu-water and  $Al_2O_3$ -water

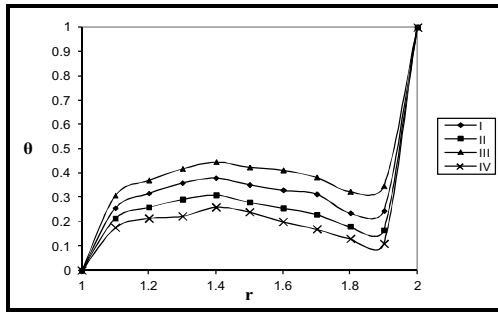


Fig. 3b. Variation of  $\theta$  with different values of  $\alpha$  (2, 4) in Cu-water and  $\text{Al}_2\text{O}_3$ -water

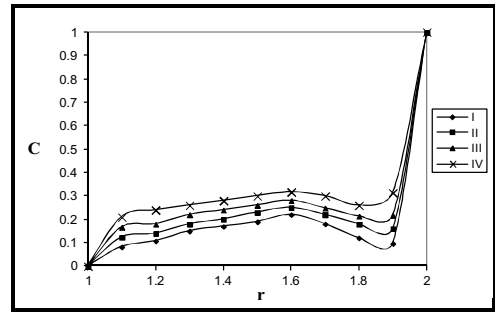


Fig. 3c. Variation of  $C$  with different values of  $\alpha$  (2, 4) in Cu-water and  $\text{Al}_2\text{O}_3$ -water

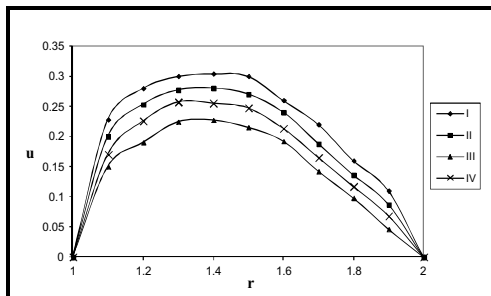


Fig. 4a. Variation of  $u$  with different values of  $\gamma$  (0.5, 1.5) in Cu-water and  $\text{Al}_2\text{O}_3$ -water

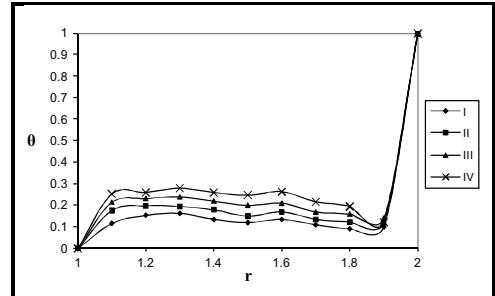


Fig. 4b. Variation of  $\theta$  with different values of  $\gamma$  (0.5, 1.5) in Cu-water and  $\text{Al}_2\text{O}_3$ -water

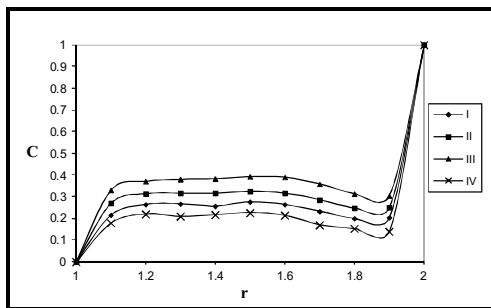


Fig. 4c. Variation of  $C$  with different values of  $\gamma$  (0.5, 1.5) in Cu-water and  $\text{Al}_2\text{O}_3$ -water

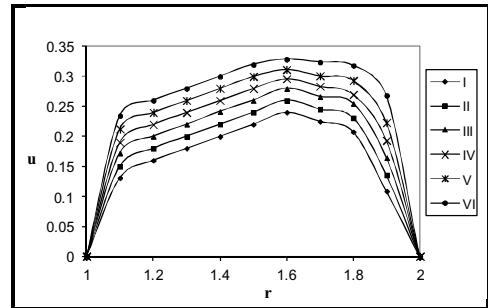


Fig. 5a. Variation of  $u$  with different values of  $\emptyset$  (0.3, 0.5, 0.7) in Cu-water and  $\text{Al}_2\text{O}_3$ -water

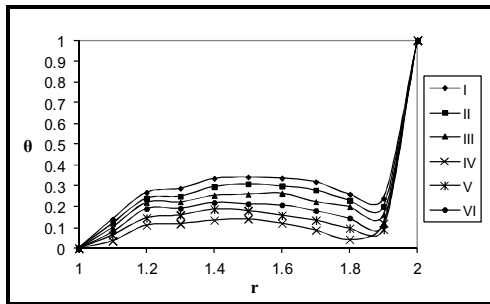


Fig. 5b. Variation of  $\theta$  with different values of  $\Phi$  (0.3, 0.5, 0.7) in Cu-water and  $\text{Al}_2\text{O}_3$ -water

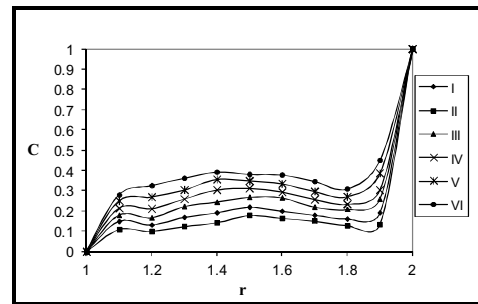


Fig. 5c. Variation of  $C$  with different values of  $\Phi$  (0.3, 0.5, 0.7) in Cu-water and  $\text{Al}_2\text{O}_3$ -water

Figs. 4a-4c represent the velocity enhancement in the generating chemical reaction case for copper-water nanofluid. In the case of  $\text{Al}_2\text{O}_3$ -water nanofluid the magnitude of the velocity enhances in generating cases. The actual temperature/actual concentration reduces in the generating case in both types of nanofluids. The magnitude of Sherwood number reduces on  $r=1$  and enhances on  $r=2$  in both generating chemical reaction case in the case of copper-water nanofluid. In the case of  $\text{Al}_2\text{O}_3$ -water nanofluid  $|Sh|$ , in the generating chemical reaction case  $|Sh|$  reduces on  $r=1$  and enhances on  $r=2$  is shown in Table 1.

Figs. 5a-5c represent that the variation of velocity, temperature and concentration with an increase in the volume fraction nanoparticles leads to an enhancement in the velocity and concentration in both types of nanofluids. In the case of temperature distribution, the actual temperature reduces in copper-water nanofluid and enhances in the  $\text{Al}_2\text{O}_3$ -water nanofluid. Also it is observed that the values of velocity and concentration in copper-water are relatively higher than those of  $\text{Al}_2\text{O}_3$ -water nanofluid, while the values of temperature in copper-water nanofluid are lesser than those of  $\text{Al}_2\text{O}_3$ -water nanofluid.

Table 1 shows that  $|Sh|$  enhances in copper-water nanofluid and reduces on  $r=1$  and  $r=2$  in  $\text{Al}_2\text{O}_3$ -water nanofluid on both the cylinders. It is also observed that  $\text{Al}_2\text{O}_3$ -water nanofluid has the highest Sherwood number on both the cylinders.

Table 1. Nusselt and Sherwood number of Cu-water and  $\text{Al}_2\text{O}_3$ -water

Properties		Cu-water		$\text{Al}_2\text{O}_3$ -water		Properties		Cu-water		$\text{Al}_2\text{O}_3$ -water	
		Nu1	Nu2	Nu1	Nu2			Sh1	Sh2	Sh1	Sh2
M	2	2.66091	12.3854	4.51228	9.08902	$\gamma$	0.5	1.54883	0.545688	2.57547	4.98648
	5	2.76328	12.3914	4.71694	9.08895		1.5	1.54883	0.546883	3.08586	5.5897
	10	2.82551	12.4579	5.68275	9.08868		-0.5	1.53852	0.548835	2.17677	-4.47219
$\alpha$	2	2.66091	12.3854	4.51228	9.08902		-1.5	1.52342	0.549945	1.85899	-4.502432
	4	7.88135	14.4868	2.63446	11.4048	$\Phi$	0.1	1.56483	0.545688	2.59064	-4.9771
$\Phi$	0.1	2.66091	12.3854	-1.65255	9.07321		0.3	1.56584	0.545975	2.45384	-4.90124
	0.3	2.04735	12.2816	0.184448	9.076297		0.5	1.56513	0.546482	2.35648	-4.8772
	0.5	2.03536	12.2039	2.0359	9.07808						
	0.7	2.02699	12.2016	4.51228	9.08902						

## References

- [1] S.U.S. Choi, J.A. Eastman, Enhancing thermal conductivity of fluids with nanoparticles, International mechanical engineering congress and exhibition, San Francisco, CA (United States), Report number: ANL/MSD/CP-84938, CONF-951135-29 ON, DE96004174, (1995) TRN: 96:001707.
- [2] A. Barletle, Combined forced and free convection with viscous dissipation in a vertical duct, *Int. J. Heat and mass transfer* 42 (1999) 2243–2253.
- [3] M.A.I. El-Shaarawi, M.A. Al-Nimir, Fully developed laminar natural convection in open ended vertical concentric annuli, *Int. J. Heat and mass transfer* 33 (1999) 1873–1884.
- [4] M.A. Al-Nimir, Analytical solutions for transient laminar fully developed free convection in vertical annuli, *Int. J. Heat and mass transfer* 36 (1993) 2388–2395.
- [5] J.R. Philip, Axisymmetric free convection at small Rayleigh numbers in porous cavities. *Int. J. Heat and mass transfer* 25 (1982) 1689–1699.
- [6] N. Putra, W. Roetzel, S.K. Das, Natural convection of nanofluids, *Heat Mass Transfer* 39(8–9) (2003) 775–784.
- [7] D. Wen, Y. Ding, Formulation of nanofluids for natural convective heat transfer applications. *Int. J. Heat Fluid Flow* 6 (2005) 855–864.
- [8] C.H. Li, G.P. Peterson, Experimental studies of natural convection heat transfer of Al<sub>2</sub>O<sub>3</sub>/DI water nanoparticle suspensions (nanofluids), *Advances in Mechanical Engineering* 2 (2010) Article ID: 742739, 49.
- [9] N. Rui, Z. Sheng-Qi, X. Ke-Qing, An experimental investigation of turbulent thermal convection in water-based alumina nanofluid. *Physics of Fluids* 23 (2011) 022005.
- [10] A.G.A. Nnanna, Experimental model of temperature-driven nanofluid, *Journal of Heat Transfer* 129 (6) (2007) 697–704.
- [11] A.J. Chamkha, E. Abu-Nada, Mixed Convection Flow in Single- and Double-Lid Driven Square Cavities Filled with Water-Al<sub>2</sub>O<sub>3</sub> Nanofluid: Effect of Viscosity Models, *European Journal of Mechanics – B/Fluids* 36 (2012) 82-96.
- [12] M. Ghalambaz, A. Behseresht, J. Behseresht and A. J. Chamkha, Effects of Nanoparticles Diameter and Concentration on Natural Convection of the Al<sub>2</sub>O<sub>3</sub>-Water Nanofluids Considering Variable Thermal Conductivity around a Vertical Cone in Porous Media. *Advanced Powder Technology* 26 (2015) 224-235.
- [13] Xiangyin Meng and Yan Li, Numerical study of natural convection in a horizontal cylinder filled with water-based alumina nanofluid, *Nanoscale Research Letters* 10 (2015) 142.